Food Chemistry 449 (2024) 139194

Contents lists available at ScienceDirect

Food Chemistry

journal homepage: www.elsevier.com/locate/foodchem

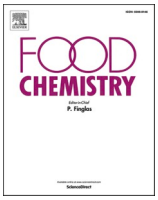

Fingerprinting of monovarietal olive oils from Argentina and Uruguay via stable isotope, fatty acid profile, and chemometric analyses

Jorge Enrique Spangenberg [a,*], Irene Lantos [b]

[a] Institute of Earth Surface Dynamics (IDYST), University of Lausanne, Geopolis Building, CH-1015 Lausanne, Switzerland
[b] Instituto de las Culturas (IDECU), Universidad de Buenos Aires & Consejo Nacional de Investigaciones Científicas y Técnicas, Moreno 350, C1091AAH Buenos Aires, Argentina

ARTICLE INFO

Keywords:
Olive oil
Traceability
IRMS
FAMEs
$\delta^{13}C$, $\delta^{2}H$ and $\delta^{18}O$

ABSTRACT

Tracing methods of non-European EVOOs commercialized worldwide are becoming crucial for effective authenticity controls. Limited analytical studies of these oils are available on a global scale, similar to those of European EVOOs. We report for the first time the fatty acid concentrations, bulk-oil $^{2}H/^{1}H$, $^{13}C/^{12}C$, and $^{18}O/^{16}O$ ratios and fatty acid $^{13}C/^{12}C$ ratios of 43 authentic monovarietal EVOOs from different geographical regions in Argentina and Uruguay. The samples were obtained from a wide range of latitudes and altitudes along an E–W profile, from lowlands near the Atlantic Ocean to the pre-Andean highlands near the Pacific Ocean. Principal component scores were used to cluster EVOOs into three groups— central-western Argentina, central Argentina, and Uruguay—based on nine stable isotope ratios and the oleic-linoleic acid concentration ratio. The bulk $^{2}H/^{1}H$ and $^{18}O/^{16}O$ values and $^{13}C/^{12}C$ of palmitoleic and linoleic acids provide good tools for differentiating these oils via linear discriminant analysis.

1. Introduction

The globalization of the food trade and the increased consumer demand for high-quality, healthy foods are increasing the importance of methods to authenticate and identify the geographical origins of edible vegetable oils (Visciano & Schirone, 2021). Olive oil is especially vulnerable to counterfeiting (Casadei et al., 2021), which, in addition to causing economic fraud, introduces potential risks of adverse health and nutritional effects to consumers. In recent decades, the cultivation of olive trees (*Olea europaea* L.), a typical Mediterranean tree from Roman times, has been expanded worldwide to temperate to arid climatic regions (Diez et al., 2015). In South America, the main countries producing high-quality extra virgin olive oils (EVOOs) are Argentina, Chile, Perú, Brazil, and Uruguay (Torres et al., 2017). Although EVOO is the primary source of fat in the Mediterranean diet, this is not the case in Argentina and Uruguay, where most of the produced olive oil is exported. Together, these two countries are the top producers and exporters of EVOO from the Americas. The United States, Brazil, China, Spain, Germany, and Japan are the main destination countries for these EVOOs. The production of EVOO increased from 10,000 t in 2001 to 34,400 t in 2022, and exports increased from 1004 t in 2001 to 26,900 t in 2022 (Supplementary Fig. S1). The steadily increasing export of South American EVOOs has raised concerns about the authenticity and geographical provenance of olive oils on the international market. Therefore, it has become increasingly important to authenticate and trace the geographical origins of non-European EVOOs to detect potential fraud in the European market. In particular, the characterization of South American EVOOs with analytical data at a resolution level similar to that available for EVOOs from EU countries is lacking. Here, to help fill this gap, we focused on the chemical and isotopic characterization of monovarietal EVOOs produced in different regions of Argentina and Uruguay (Fig. 1).

More than twenty olive varieties are grown in Argentina and Uruguay. They were introduced from traditional oil-producing countries in the Mediterranean Basin. The main varieties include Arbequina, Picual (Spain), Coratina, and Frantoio (Italy) and, to a lesser extent, Manzanilla, Leccino, Hojiblance (Spain), and Koroneiki (Greece) (Ministerio de Ganadería, Agricultura y Pesca, 2020). The only known native Argentinian variety is Arauco, which is mainly grown in Mendoza Province (Banco, Trentacoste, & Monasterio, 2021). Although in Argentina and Uruguay, some medium- to small-sized olive groves are dominated by trees older than 100 years, the expansion of modern oliviculture in the 2000s resulted in the introduction of a large proportion of young orchards. Therefore, the production and export of EVOO are

* Corresponding author.
E-mail address: Jorge.Spangenberg@unil.ch (J.E. Spangenberg).

https://doi.org/10.1016/j.foodchem.2024.139194
Received 9 January 2024; Received in revised form 18 March 2024; Accepted 28 March 2024
Available online 30 March 2024

expected to increase considerably in the coming years. It is highly important to develop reliable identification and classification methods for distinguishing between extra virgin olive oils from these South American countries based on their origins and cultivars and for potentially differentiating between harvest years in the future.

Depending on the olive genotype and its environmental plasticity, the molecular and isotopic compositions of derived EVOO may differ statistically significantly when an olive cultivar is grown in the Southern Hemisphere rather than its original Mediterranean region (Spangenberg, 2016). For example, Arbequina EVOOs from Argentina, Brazil, and Uruguay have consistently lower oleic acid contents and higher palmitic and linoleic acid contents than oils from the original Arbequina regions in Spain (Borges et al., 2017; Torres et al., 2017). Furthermore, the bulk and molecular stable isotope ratios of carbon, hydrogen, and oxygen ($^{13}C/^{12}C$, $^{2}H/^{1}H$, and $^{18}O/^{16}O$, respectively, expressed as $\delta^{13}C$, $\delta^{2}H$, and $\delta^{18}O$) of plants and their products are linked to the isotopic compositions of atmospheric CO_2 and plant-available waters (soil water, groundwater, rainwater, irrigation water). The primary photosynthetic and biosynthetic fractionations control these relationships, which are strongly influenced by local environmental parameters and agricultural practices (O'Leary, Madhavan, & Paneth, 1992; Schmidt, Werner, & Eisenreich, 2003; Schmidt, Werner, & Rossmann, 2001). Therefore, several researchers have used stable isotopic techniques based on the $\delta^{13}C$, $\delta^{2}H$, and $\delta^{18}O$ values of bulk oil and bulk fractions (e.g., sterols, aliphatic alcohols) for the characterization, authentication, and tracing of the geographical origins of EVOOs in European countries (e.g., Angerosa et al., 1999; Aramendía et al., 2010; Bontempo et al., 2009; Camin et al., 2010; Camin et al., 2010; Iacumin, Bernini, & Boschetti, 2009). Olive oils from the Italian Tyrrhenian and Adriatic coasts for each year (2005–2007) could be distinguished mainly based on their bulk $\delta^{2}H$ values (Bontempo et al., 2009).

Compound-specific $\delta^{13}C$ analysis, alone (Spangenberg, 2016; Spangenberg, Macko, & Hunziker, 1998; Spangenberg & Ogrinc, 2001) or combined with compound-specific $\delta^{2}H$ analysis (Bontempo et al., 2019; Paolini, Bontempo, & Camin, 2017), has been shown to significantly improve the authentication of olive oils. However, stable isotope characterization of olive oils from the Southern Hemisphere is lacking. Two studies attempted to start filling this gap (Bontempo et al., 2019; Spangenberg, 2016) and presented the first stable isotopic data of a few commercially available EVOOs from Argentina and Uruguay. The analyzed oils had no clear geographical origins or olive variety information. Despite these limitations, differences between the southern and northern hemispheres were observed mainly in the $\delta^{2}H$ and less significant $\delta^{18}O$ values of the bulk oils. Given the different geographical and climatic conditions of the olive growing regions in Argentina (relatively high altitude) and Uruguay (coastal lowlands), it could be hypothesized that the EVOOs from these neighboring countries may be discriminated by their chemical and isotopic composition.

The main goal of this study was to compare the fatty acid profiles and isotopic compositions of EVOOs from Argentina and Uruguay and determine whether the potential differences can be used for traceability. The specific objectives were to (1) determine the bulk-oil $^{13}C/^{12}C$, $^{2}H/^{1}H$, and $^{18}O/^{16}O$ ratios, fatty acid profiles, and $^{13}C/^{12}C$ ratios of the main fatty acids (in biosynthetic order: palmitic, palmitoleic, stearic, oleic and linoleic acids) of EVOOs derived from growing sites covering a range of latitudes, altitudes, and climates in Argentina and Uruguay; (2) identify the most suitable parameters for geographically authenticating these EVOOs; and (3) evaluate whether differences between cultivars can impede efforts toward geographical identification based on these parameters.

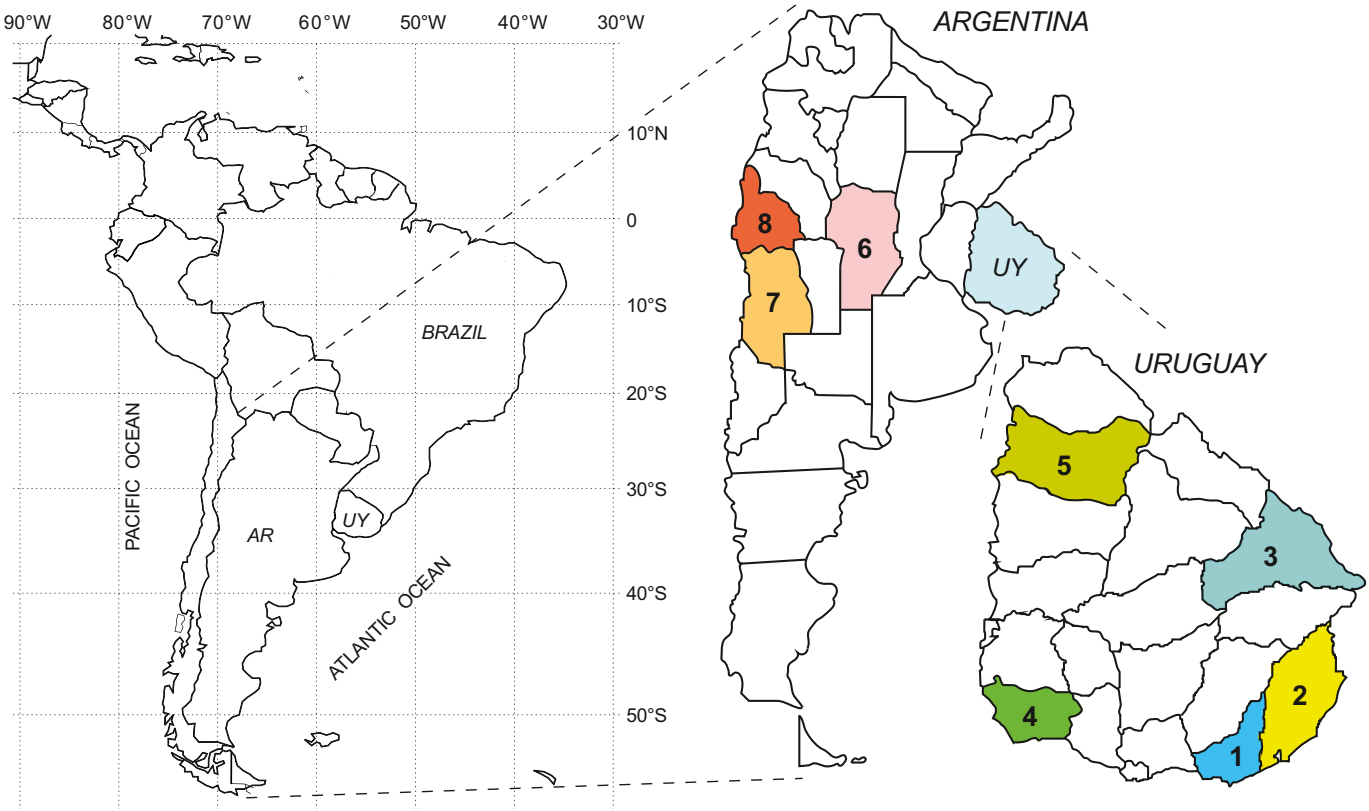

Fig. 1. Regions in Argentina (AR) and Uruguay (UY) where the domestic monovarietal virgin olive oils were collected. They are ordered from east to west and south to north.
1 - Maldonado, 2 - Rocha, 3 - Cerro Largo, 4 - Colonia, 5 - Salto, 6 - Córdoba, 7 - Mendoza, 8 - San Juan.

2. Materials and methods

2.1. Samples

A total of 43 samples of authentic EVOOs from three different regions in Argentina and eight in Uruguay with various geographical and climatic (i.e., geoclimatic) conditions produced during the 2017 season from different single cultivars were analyzed (Fig. 1 and Supplementary Table S1). Oil samples were collected from 18 organic farms along an east–west profile from the Atlantic coast lowland of southeastern Uruguay, passing through the lowland grasslands and agricultural fields of eastern Córdoba Province in central Argentina to the fertile valleys of the pre-Andean highlands (Andean Precordillera) in San Juan and Mendoza provinces in central-western Argentina (Fig. 1). The Argentinian oils ($n = 20$) come from sites with latitudes and altitudes within 31.29–33.00S and 600–840 masl, respectively; the Uruguayan oils ($n = 23$) come from areas with latitudes and altitudes within 31.19–34.45S and 30–140 masl, respectively (Table S1). The samples cover an altitude range of 810 m and include temperate oceanic (Cfb), humid subtropical (Cfa), cold and hot arid desert (Bwk, Bwh) climatic types (Table S1). The geographical location and agroclimatic parameters (altitude, latitude, longitude, mean annual temperature, sunshine duration, precipitation, and irrigation type and cultivar) for each sample site are given in Table S2. The oil samples were collected in duplicate in closed 7 mL dark amber glass vials with PTFE-lined solid screw caps and no headspace. These sample vials were stored at 4 °C until they were air-shipped via FedEx from Buenos Aires to the University of Lausanne on ice packs and then kept at 4 °C until analysis. Irrigation water samples ($n = 8$) were collected from four Argentinian sites and two Uruguayan sites (Table S4).

2.2. Stable isotope analysis of bulk EVOOs

The $^{13}C/^{12}C$ ratios of the bulk oil samples were determined by elemental analysis/isotope ratio mass spectrometry (EA/IRMS) using a Carlo Erba 1108 analyzer (Fisons Instruments, Milan, Italy) connected to an isotope ratio mass spectrometer (Delta V Plus, Thermo Fisher Scientific, Bremen, Germany). The measurements of $^{2}H/^{1}H$ and $^{18}O/^{16}O$ were performed using high-temperature conversion-elemental analysis/isotope ratio mass spectrometry (TC-EA/IRMS) by coupling a TC elemental analyzer to a MAT 253 isotope ratio mass spectrometer (both from Thermo Fisher Scientific). Details of the instrumental conditions were reported previously (Spangenberg, 2016). The measurements were performed in duplicate and repeated twice or thrice (i.e., $n = 4$ to 6). Aliquots of 100–400 μg of oil were weighed in tin capsules to analyze the C isotope composition and in silver capsules to analyze H and O isotope compositions. Before analysis, the silver capsules containing the oil samples or standards were kept for >24 h in a vacuum desiccator with silica gel. Separate TC-EA pyrolysis with different aliquots of the oil samples was used for H and O isotope analyses.

The measured isotope ratios are reported in the delta (δ) notation corresponding to the relative deviations of the molar ratio (R) of the heavy (^{h}E, i.e., ^{13}C, ^{2}H, or ^{18}O) to light (^{l}E, i.e., ^{12}C, ^{1}H, or ^{16}O) isotopes in the samples from those in international standards, as shown in the following equation:

$$\delta^{h}E_{sample} = \frac{R\left(^{h}E/^{l}E\right)_{sample}}{R\left(^{h}E/^{l}E\right)_{standard}} - 1$$

The $\delta^{13}C$ values are expressed relative to the Vienna Pee Dee Belemnite limestone (VPDB), and the $\delta^{2}H$ and $\delta^{18}O$ values are relative to Vienna Standard Mean Ocean Water (VSMOW). The International System of Units (SI) unit for the δ-values is the urey (symbolized Ur), according to the guidelines and recommendations of the IUPAC—Commission on Isotopic Abundances and Atomic Weights (Brand & Coplen, 2012). The δ-values were multiplied by 1000 and reported in milliurey (mUr) rather than the deprecated per mil (‰), which is not an SI unit. The measured δ values (i.e., $\delta^{13}C$, $\delta^{2}H$, and $\delta^{18}O$ values based on working gas cylinders of CO_2, H_2, and CO, respectively) were normalized to the VPDB-LSVEC and VSMOW-SLAP scales using three- or four-point calibration with international reference materials (RMs). The RMs and the recommended consensus values (Schimmelmann et al., 2020) used for scale anchors and quality control of $\delta^{13}C$ values were glycine USGS64, USGS65 and USGS66 ($\delta^{13}C$ values: −40.81, −20.29 and − 0.67 mUr, respectively); the RMSs used for $\delta^{2}H$ and $\delta^{18}O$ values were an olive oil from Sicily USGS84 ($\delta^{2}H$: −140.4 mUr, $\delta^{18}O$: +26.36 mUr), a peanut oil from tropical Vietnam ($\delta^{2}H$: −207.4 mUr, $\delta^{18}O$: +18.76 mUr), a corn oil from the USA ($\delta^{2}H$: −168.1 mUr, $\delta^{18}O$: +20.11 mUr), polyethylene foil IAEA-CH-7 ($\delta^{2}H$: −99.2 mUr) and benzoic acids IAEA-601 and IAEA-602 ($\delta^{18}O$: +23.14 and + 71.28 mUr, respectively). The repeatability and intermediate precision of the C, H, and O isotope values were determined by the standard deviation of separately replicated analyses ($n = 4$ to 6) of RMs (not used in the calibration of the analytical sequence). These values were better than ±0.1 mUr for $\delta^{13}C$, ±1.0 mUr for $\delta^{2}H$, and ± 0.3 mUr for $\delta^{18}O$.

2.3. Stable isotope analysis of irrigation water

Hydrogen and oxygen isotope analyses of water samples were performed by wavelength-scanned cavity ring-down spectroscopy (WS-CRDS, Picarro L-1120i; Picarro Inc., Santa Clara, CA, USA), as described previously (Spangenberg, 2012). The reproducibility as assessed by replicate ($n = 2$–4) analysis was better than 0.3 mUr and 0.1 mUr (1 s) for the $\delta^{2}H$ and $\delta^{18}O$ values, respectively.

2.4. Separation and transesterification of fatty acids

The total fatty acids (mainly triglyceride-bonded and traces of free acids) were transesterified to produce fatty acid methyl esters (FAMEs) by an alkali-catalyzed methanolysis reaction (Commission Regulation (EC), n.d.). An aliquot of 0.1 g of oil was weighed and placed in a 5 mL vial with a PTFE-lined screw cap, and 2 mL of hexane and 0.2 mL of 2 M methanolic potassium hydroxide solution were added. The vial was closed and shaken for 1 min at room temperature, followed by layer separation until the upper hexane solution containing the FAMEs became clear, and the aliquots were injected into the gas chromatographic system.

2.5. Fatty acid characterization and concentrations

The analyses were performed following the procedures described in Spangenberg (2016). Briefly, chemical characterization of FAMES was performed via GC/MS using an Agilent (Palo Alto, CA, USA) 6890 gas chromatograph connected to an Agilent 5973 mass selective detector. The FAMEs were separated using an HP-FFAP column (50 m 0.20 m i.d.) coated with a 0.33 μm nitroterephthalic acid-modified polyethylene glycol stationary phase. The mass scan was in the m/z 45–500 range. The concentrations of the FAMEs were determined by gas chromatography/flame ionization detection (GC/FID) using an Agilent Technologies (2850 Centerville Road, Wilmington, DE, USA) 7890B GC system equipped with a 7693 A automated injection system and a flame ionization detector.

2.6. Carbon isotope analysis of individual fatty acids

The $\delta^{13}C$ values of the main oil fatty acids (i.e., 16:0, 16:1, 18:0, 18:1, and 18:2) were determined by GC/combustion/isotope ratio MS (GC/C/IRMS) using an Agilent 6890 GC instrument connected to a Delta V Plus isotope ratio mass spectrometer via a Combustion III interface. The GC settings were the same as those used for GC/MS. Details on the GC/C/IRMS system used and its operation are detailed in Spangenberg (2016). For calibration of the measured $\delta^{13}C$ values, aliquots of freshly prepared

solutions of the RMs icosanoic FAMEs USGS70, USGS71, and USGS72 (δ^{13}C values: −30.25, −10.50, and − 1.54 mUr, respectively; Schimmelmann et al., 2020) in hexane were injected daily. A mass balance equation was used to correct the isotopic shift that occurred due to the carbon introduced in fatty acid methylation (Spangenberg et al., 1998). Each oil sample was analyzed three to six times for its fatty acid δ^{13}C values. The standard deviations for repeatability ranged between 0.05 and 0.2 mUr for the main FAMEs.

2.7. Statistical analysis

Statistical analyses were performed using SPSS software (IBM SPSS Statistics version 28.0.1.1, IBM Corp., Armonk, NY, USA). The variables under consideration included three bulk oil stable isotope ratios (δ^{13}C, δ^{2}H, δ^{18}O), 11 fatty acid concentrations and parameters (total saturated fatty acids (SFAs), total monounsaturated fatty acids (MUFAs), total polyunsaturated fatty acids (PUFAs), the concentration ratio of oleic/linoleic acid, linoleic/linolenic acid, MUFA/PUFA, PUFA/SFA, and δ^{13}C values of the five main fatty acids). Descriptive analysis and analysis of variance (one-way ANOVA) with the eight geographical sites of the EVOOs as the main factor were used to establish the differences in the mean values between sites. The significance of the comparisons was assessed by different post hoc tests, including Tukey's (HSD, honestly significant difference), Fisher's (LSD, least significant difference), and Duncan's tests. The results of the HSD test were compared with those of the less conservative LSD test to ensure that some subtle mean differences between sites were not overlooked and to define the more homogeneous groups of EVOO sites. The cutoff for statistical significance was set to $P < 0.05$. We present the results of Tukey HSD analyses, as it is considered the preferred test when comparing multiple groups. Pearson correlation coefficients (r values) and two-tailed Student's tests were used to measure linear bivariate correlations between the variables. Graphics were prepared using DeltaGraph V7.1.3 (Red Rock Software Inc., Salt Lake City, UT, USA), Adobe Illustrator 2022 V27.1.1 (Adobe Systems Inc., CA, USA), and 2022 Microsoft PowerPoint V16.69.1. Three-dimensional scatterplots were prepared with Excel macros (https://www.doka.ch/Excel3Dscatterplot.htm).

2.7.1. Principal component analysis (PCA)

Principal component analysis (PCA) was used for dimensionality reduction and as an exploratory (unsupervised) technique to cluster the isotopic variables and fatty acid concentration variables within a limited number of independent variables (principal components) and explore the separation of potential groups of EVOO samples. The variables subjected to PCA were chosen according to the significant Pearson's correlations among them and statistically significant mean differences according to the one-way ANOVA results with independent factors in the olive growing regions in Argentina and Uruguay.

2.7.2. Linear discriminant analysis (LDA)

Linear discriminant analysis (LDA) was used as a supervised technique for the classification of oil samples and to confirm the grouping of the sites of EVOO samples suggested by PCA, one-way ANOVAs, and scatterplots. LDA maximizes the variance between groups and minimizes the variance within the groups. A forward stepwise discriminant procedure was used to extract the most discriminant subset of variables separating EVOO regions based on Wilks' lambda criterion and F-statistics. The predictive ability of the LDA model was evaluated by the leave-one-out cross-validation (LOOCV) method.

2.7.3. General linear model (GLM)

The average isotopic values of bulk oils and individual fatty acids were subjected to two-way ANOVA using the general linear model (GLM procedure), considering separately the two main grouped EVOO regions revealed by PCA and LDA (i.e., San Juan and Mendoza provinces in northwestern central Argentina and Uruguayan sites) and olive cultivars (Arauco, Arbequina, and Frantoia). The main effects and their interactions were studied for all variables.

3. Results and discussion

3.1. Stable isotope ratios of bulk oils

The δ^{13}C values for all the EVOO samples ranged from −31.6 to −28.6 mUr, which was related to the fact that the olive tree is a C_3 plant, while the δ^{2}H and δ^{18}O values varied from −203.0 to −146.0 mUr and 19.4 to 26.5 mUr, respectively. Statistically significant differences ($P < 0.05$, one-way ANOVA with post hoc Tukey HSD test) existed between samples from different growing areas in terms of the δ^{13}C, δ^{2}H, and δ^{18}O values of the bulk EVOOs (Table S3). Details on the variations in the bulk isotope ratios for the eight sites are shown in Table 1 and as boxplots in Fig. S2A. The average $\delta^{13}C_{bulk}$ values from the eight different EVOO production areas varied within a narrow range from −30.7 to −29.7 mUr, with lower values in regions on the coastal lowlands of eastern Uruguay (regions 1, 2, and 3, Maldonado, Rocha, and Cerro Largo departments, respectively) and higher values in the northwestern region of Uruguay (region 5, Salto Department). This trend can be explained by the fact that at all latitudes, high-altitude C_3 plants show less carbon isotope discrimination (i.e., higher δ^{13}C values) than comparable lowland plants (Körner, Farquhar, & Wong, 1991).

The average $\delta^{13}C_{bulk}$ values decreased in the order 5 (Salto) > 6 (Córdoba) > 8 (San Juan) > 4 (Colonia) > 1 (Maldonado) ≈ 2 (Rocha) ≈ 3 (Cerro Largo) (Table 1). Region 5 showed significant differences from regions 1 to 3. No significant differences existed between regions 1–4 and 6–8. δ^{13}C values are linked to photosynthetic yield, which is closely related to the geoclimatic characteristics of the growing/production area, including irradiance, atmospheric CO_2 concentration, temperature, and soil water availability. These parameters impact ~~the~~ CO_2 stomatal conductance and induce changes in the δ^{13}C of plant organs and products (e.g., O'Leary et al., 1992). The $\delta^{13}C_{bulk}$ value alone had relatively limited discriminatory power between the individual EVOO sites; however, the EVOOs from Salto (site 5) are significantly different ($P < 0.05$) from those from the Uruguayan coastal regions 1–3 and similar to the Argentinian oils from regions 6 to 8 (Table 1).

The δ^{2}H values provided better differentiation between the Argentinian and Uruguayan regions (Tables 1 and S3, Fig. S2A). The lowest δ^{2}H values were measured in oils from regions 7 and 8 (Mendoza and San Juan, central-western Argentina), the highest δ^{2}H values were measured in region 6 (Córdoba, central Argentina), and intermediate values were measured in the Uruguayan EVOOs (regions 1–5). The average δ^{2}H values per growing region showed a southeast to northwest geographical trend in the order of 6 > 1 ≈ 2 ≈ 3 ≈ 4 > 5 ≈ 7 ≈ 8 (Table 1). Among them, sites 7 and 8 showed significant differences from regions 1–4 and 6 and a marginal but not statistically significant difference from region 5. Region 6 significantly differed from regions 5, 7, and 8. The average δ^{18}O values show a trend of 6 > 8 ≈ 4 > 2 > 1 ≈ 7 > 3 > 5. Regions 3 and 5 were significantly different from region 6. The difference between Uruguayan regions 1–4 and region 5 was related to the distance to the coast, showing an isotopic gradient of continentality, i.e., loss of the heavy isotopes through consecutive precipitation events. The water vapor that remains becomes progressively depleted in heavy isotopes, yielding precipitation with lower δ^{2}H and δ^{18}O values (Rozanski, Araguás-Araguás, & Gonfiantini, 1993). The samples from Córdoba (region 6) had exceptionally high values for both δ^{2}H and δ^{18}O. The local climatic conditions may explain this difference. Córdoba is within the central Argentinian climatic region of dry Pampa, with a hot (18–30 °C) humid subtropical climate (Cwa). The relatively high local temperature and humidity increase ~~the~~ soil/plant evapotranspiration, which leads to ^{2}H and ^{18}O enrichment (i.e., higher δ^{2}H and δ^{18}O values) in plant tissues and products (e.g., da Silveira Lobo Sternberg, 1989). The samples from Mendoza and San Juan (regions 7 and 8) had the lowest δ^{2}H values with intermediate δ^{18}O. Both provinces belong to the

Table 1
Bulk oil isotopic ratios (mUr) and fatty acid concentrations (%), concentration ratios, and individual $\delta^{13}C$ values.

Region	1	2	3	4	5	6	7	8
(*N*)	(10)	(5)	(3)	(3)	(2)	(4)	(10)	(6)
$\delta^{13}C_{bulk}$	−30.63 ± 0.29^{a}	−30.67 ± 0.40^{a}	−30.62 ± 0.39^{a}	−29.86 ± 0.52^{ab}	−29.14 ± 0.73^{b}	−29.68 ± 0.12^{ab}	−29.98 ± 0.42^{ab}	−29.72 ± 0.90^{ab}
$\delta^{2}H_{bulk}$	−162.9 ± 4.3^{bc}	−164.3 ± 3.4^{bc}	−163.3 ± 6.3^{bc}	−165.2 ± 1.4^{bc}	−175.4 ± 4.2^{ab}	−152.2 ± 4.7^{c}	−189.2 ± 10.5^{a}	−191.2 ± 9.3^{a}
$\delta^{18}O_{bulk}$	21.17 ± 0.63^{ab}	21.45 ± 0.43^{ab}	20.56 ± 0.45^{a}	21.81 ± 0.45^{ab}	20.17 ± 0.19^{a}	23.60 ± 0.31^{b}	21.16 ± 2.19^{ab}	21.94 ± 1.13^{ab}
C16:0	14.81 ± 1.45^{a}	15.51 ± 2.99^{a}	17.77 ± 2.26^{a}	16.50 ± 1.55^{a}	18.07 ± 1.78^{a}	16.34 ± 1.75^{a}	15.28 ± 2.51^{a}	17.04 ± 3.36^{a}
C16:1	1.13 ± 0.43^{a}	1.25 ± 0.90^{a}	1.41 ± 0.83^{a}	1.73 ± 0.14^{a}	1.85 ± 0.29^{a}	1.44 ± 0.23^{a}	1.42 ± 0.45^{a}	1.59 ± 0.58^{a}
C17:0	0.14 ± 0.08^{ab}	0.10 ± 0.05^{ab}	0.08 ± 0.03^{a}	0.20 ± 0.11^{b}	0.07 ± 0.03^{a}	0.06 ± 0.01^{a}	0.07 ± 0.02^{a}	0.09 ± 0.03^{ab}
C17:1	0.29 ± 0.20^{a}	0.17 ± 0.06^{a}	0.19 ± 0.13^{a}	0.33 ± 0.29^{a}	0.16 ± 0.09^{a}	0.19 ± 0.08^{a}	0.14 ± 0.05^{a}	0.21 ± 0.09^{a}
C18:0	1.50 ± 0.36^{a}	1.29 ± 0.27^{a}	1.80 ± 0.64^{a}	1.43 ± 0.26^{a}	1.10 ± 0.08^{a}	1.21 ± 0.34^{a}	1.46 ± 0.15^{a}	1.70 ± 0.59^{a}
C18:1	74.82 ± 3.16^{a}	72.74 ± 7.01^{a}	65.32 ± 1.86^{a}	70.21 ± 1.76^{a}	70.91 ± 4.49^{a}	71.28 ± 2.27^{a}	71.34 ± 5.13^{a}	66.44 ± 6.66^{a}
C18:2	6.10 ± 1.91^{a}	7.57 ± 3.16^{ab}	12.14 ± 0.60^{b}	8.59 ± 0.58^{ab}	6.89 ± 2.45^{ab}	8.63 ± 2.88 ^{ab}	9.08 ± 2.45^{ab}	11.56 ± 3.26^{ab}
C18:3	0.56 ± 0.14^{a}	0.71 ± 0.13^{a}	0.64 ± 0.09^{a}	0.46 ± 0.04^{a}	0.51 ± 0.03^{a}	0.54 ± 0.20^{a}	0.60 ± 0.10^{a}	0.84 ± 0.46^{a}
C20:0	0.27 ± 0.07^{a}	0.31 ± 0.12^{a}	0.29 ± 0.08^{a}	0.29 ± 0.07^{a}	0.20 ± 0.01^{a}	0.28 ± 0.17^{a}	0.28 ± 0.06^{a}	0.26 ± 0.07^{a}
C20:1	0.29 ± 0.10^{a}	0.33 ± 0.14^{a}	0.30 ± 0.16^{a}	0.23 ± 0.06^{a}	0.15 ± 0.02^{a}	0.18 ± 0.04^{a}	0.24 ± 0.06^{a}	0.21 ± 0.08^{a}
C22:0	0.08 ± 0.06^{a}	0.13 ± 0.09^{a}	0.06 ± 0.02^{a}	0.05 ± 0.01^{a}	0.07 ± 0.02^{a}	0.05 ± 0.01^{a}	0.09 ± 0.04^{a}	0.07 ± 0.04^{a}
SFA	16.80 ± 1.38^{a}	17.25 ± 2.90^{a}	20.00 ± 1.73^{a}	18.41 ± 1.82^{a}	19.52 ± 1.70^{a}	17.86 ± 1.58^{a}	17.17 ± 2.53^{a}	19.16 ± 2.96^{a}
MUFA	76.54 ± 2.75^{a}	74.48 ± 6.03^{a}	67.22 ± 1.31^{a}	72.50 ± 1.37^{a}	73.08 ± 4.12^{a}	73.08 ± 2.20^{a}	73.15 ± 4.71^{a}	68.45 ± 6.23^{a}
PUFA	6.66 ± 1.97^{a}	8.24 ± 3.22^{a}	12.78 ± 0.65^{a}	8.92 ± 0.76^{a}	7.40 ± 2.42^{a}	8.35 ± 4.13^{a}	9.68 ± 2.43^{a}	12.10 ± 4.26^{a}
Oleic/Linoleic	13.56 ± 5.05^{a}	11.51 ± 4.70^{a}	5.38 ± 0.20^{a}	8.19 ± 0.42^{a}	11.10 ± 4.59^{a}	9.11 ± 3.48^{a}	8.33 ± 2.02^{a}	6.58 ± 3.66^{a}
MUFA/PUFA	12.60 ± 4.58^{a}	10.23 ± 3.96^{a}	5.27 ± 0.23^{a}	8.17 ± 0.58^{a}	10.52 ± 3.99^{a}	12.55 ± 10.45^{a}	7.95 ± 1.84^{a}	7.31 ± 5.83^{a}
PUFA/SFA	0.40 ± 0.11^{a}	0.47 ± 0.10 ^{a}	0.64 ± 0.08 ^{a}	0.49 ± 0.09 ^{a}	0.38 ± 0.09^{a}	0.48 ± 0.25^{a}	0.58 ± 0.08^{a}	0.62 ± 0.18^{a}
Linoleic/Linolenic	11.03 ± 3.12^{a}	11.15 ± 3.63^{a}	19.30 ± 2.19^{a}	18.70 ± 2.99^{a}	13.70 ± 5.70^{a}	20.19 ± 11.53^{a}	15.45 ± 5.39^{a}	14.34 ± 5.10^{a}
$\delta^{13}C_{16:0}$	−32.67 ± 0.38^{ab}	−32.75 ± 0.71^{a}	−32.40 ± 0.85^{ab}	−31.01 ± 0.75^{b}	−31.49 ± 0.47^{ab}	−31.61 ± 0.57^{ab}	−32.42 ± 0.94^{ab}	−31.99 ± 0.94^{ab}
$\delta^{13}C_{16:1}$	−32.83 ± 0.54^{ab}	−33.03 ± 0.33^{a}	−32.80 ± 0.67^{ab}	−31.90 ± 0.57^{ab}	−31.70 ± 0.01^{ab}	−31.40 ± 1.09^{b}	−31.59 ± 0.54^{ab}	−31.54 ± 1.92^{b}
$\delta^{13}C_{18:0}$	−33.61 ± 0.89^{ab}	−33.29 ± 0.49^{ab}	−34.38 ± 0.44^{a}	−32.50 ± 0.22^{bc}	−31.48 ± 0.08^{c}	−33.91 ± 0.54^{ab}	−32.94 ± 0.72^{abc}	−32.89 ± 1.10^{abc}
$\delta^{13}C_{18:1}$	−31.44 ± 0.60^{ab}	−31.26 ± 0.38^{ab}	−31.85 ± 0.67^{a}	−30.95 ± 1.28^{ab}	−30.01 ± 0.69^{b}	−30.84 ± 0.48^{ab}	−30.84 ± 0.50^{ab}	−30.43 ± 0.92^{ab}
$\delta^{13}C_{18:2}$	−33.40 ± 0.64^{a}	−33.82 ± 0.42^{a}	−32.36 ± 1.45^{a}	−32.29 ± 1.11^{a}	−32.31 ± 0.49^{a}	−33.08 ± 1.15^{a}	−33.50 ± 0.99^{a}	−32.97 ± 0.59^{a}

Notes: Authentic EVOOs from regions in Uruguay and Argentina (1–5 and 6–8, respectively, shown in Fig. 1). Values are given as means ± standard deviations of independent oil samples (*N*) from growing sites within the different regions. Means with different lowercase letters in the same row are significantly ($P < 0.05$) different based on Tukey HSD test.

Cuyo central-western Argentinian climatic region with latitudes coinciding with the subtropical high and characterized by cold to hot arid desert climates (Bwk, Bwh; Table S1). This region receives large inflows of isotopically light Andean snowmelt through rivers and associated groundwaters that sustain one of the largest irrigated agricultural regions in South America (Jobbágy, Nosetto, Villagra, & Jackson, 2011), with ~400 km^2 of olive orchards and ~ 2000 km^2 of vineyards in the provinces of San Juan and Mendoza. The low δ^2H values in regions 7 and 8 (Table 1) are explained mainly by the effect of continentality on the precipitation of Pacific Ocean humidity in Andean precipitation. However, the potentially lower $\delta^{18}O$ values may have been masked by ^{18}O enrichment during the interaction and isotopic exchange of groundwater and minerals (carbonates, silicates, sulfates), which would affect the $\delta^{18}O$ values and not the δ^2H values (Spangenberg, Dold, Vogt, & Pfeifer, 2007). The δ^2H (and $\delta^{18}O$) values provide better geographical discrimination of plant products. This is due to the close link between the variations in δ^2H values (and a much poorer relationship for $\delta^{18}O$ values) of plant materials and patterns in precipitation (Roden, Lin, & Ehleringer, 2000), which is particularly true in areas with a deep groundwater table, where groundwater has a negligible effect on soil moisture. Shallow groundwater may be an important source of water for crops (i.e., olive trees) in the highland grasslands of Mendoza and San Juan and coastal areas of Uruguay. Isotopic fractionation does not occur during water uptake and transport in roots and stems until the water reaches the tissues or organs (Roden et al., 2000). In some plant organs (e.g., leaves), different fractionation processes occur, including transpiration and biochemical fractionation during photosynthesis (i.e., −171 mUr δ^2H compared to the surrounding water, Yakir & DeNiro, 1990) and the synthesis of organic molecules in plant tissues and organs from substrate sugars (Roden et al., 2000). The $\delta^{18}O$ values of the EVOOs are less variable than the δ^2H values (δ^2H values covered a range of 57 mUr compared to 7.1 mUr for $\delta^{18}O$ values). This almost 10% higher hydrogen isotope fractionation than oxygen isotope fractionation is explained by the relative mass difference between the light and heavy isotopes (100% for ^2H-^1H and 12.5% for ^{18}O-^{16}O). Additionally, organic oxygen may originate from other sources, such as CO_2, rather than from water. However, it was shown that CO_2 oxygen undergoes complete isotopic exchange with water oxygen during the synthesis of cellulose (Yakir & DeNiro, 1990).

δ^2H was highly positively correlated ($P < 0.01$) with latitude and MAT, MARH, and MAP and negatively correlated with longitude, altitude, and MAI; $\delta^{18}O$ was only correlated ($P < 0.05$) with altitude (Fig. S3). $\delta^{13}C_{bulk}$ was negatively correlated with latitude, annual humidity, and precipitation and positively correlated with longitude, altitude, and yearly sunshine hours (Fig. S3). The negative $\delta^{13}C_{bulk}$-latitude correlation is explained by decreased ^{13}C discrimination (i.e., higher $\delta^{13}C$ values) associated with the latitudinally decreasing temperature at similar atmospheric pressures (Körner et al., 1991). The 3D scatterplot of the bulk isotopes shows that EVOOs from different regions in Argentina (7 and 8) and Uruguay (1 and 3) were grouped, while others had a certain degree of differentiation (Fig. 2A). These results are in line with those reported, which showed that the combined $\delta^{13}C$, δ^2H, and $\delta^{18}O$ values of bulk oils allow for the distinction of EVOOs from northern Italy from those of southern Italy (Camin, Larcher, Perini, et al., 2010) and for some geographical grouping of EVOOs from different regions in Europe (Camin, Larcher, Nicolini, et al., 2010).

The δ^2H and $\delta^{18}O$ values in the bulk oil were correlated ($P < 0.01$) but were not correlated with $\delta^{13}C$ ($P > 0.05$). The regression equation

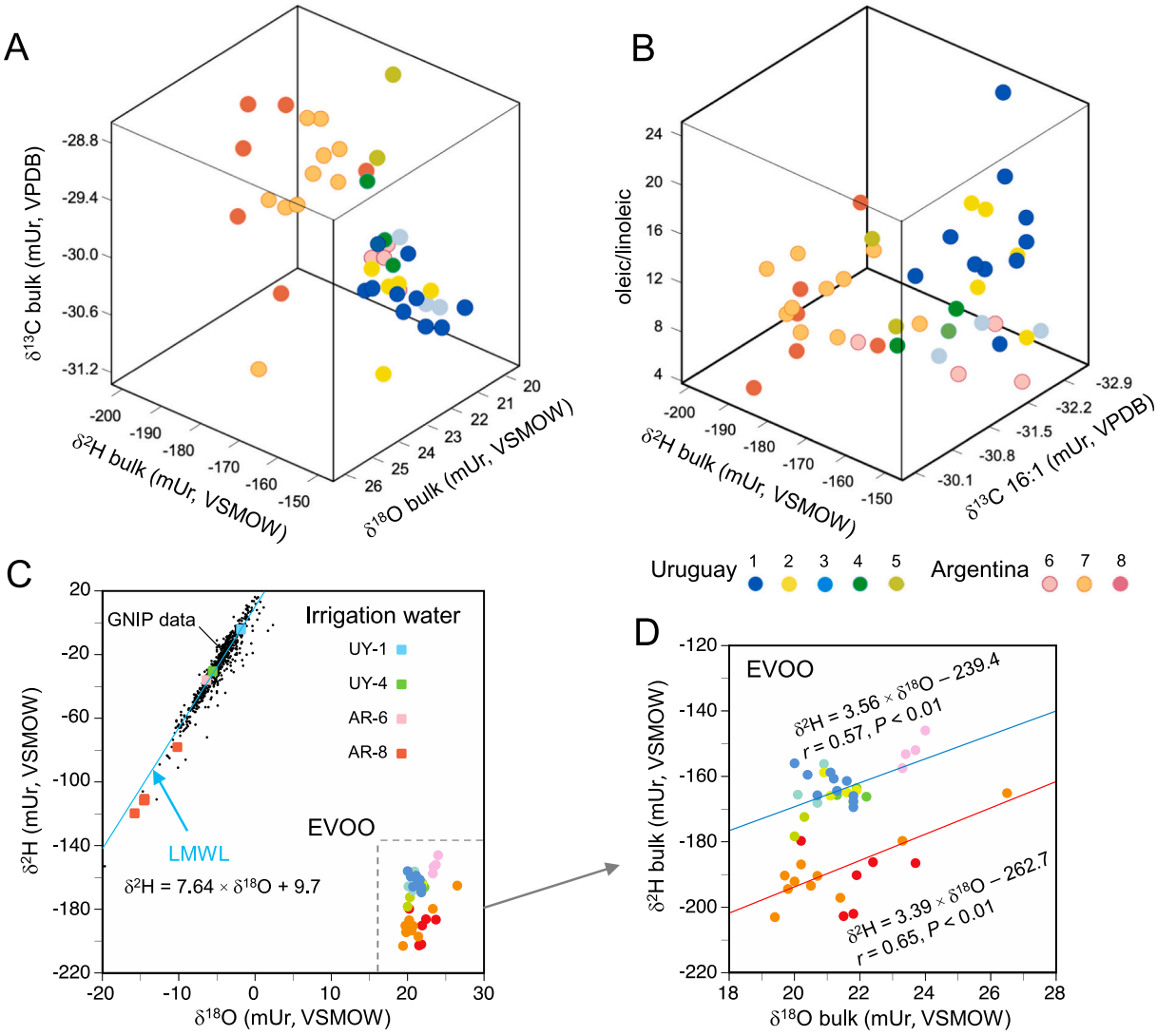

Fig. 2. Differentiation of the EVOOs according to their geographical origin in three dimensional scatter plots of d^2H_{bulk}-$d^{18}O_{bulk}$-$d^{13}C_{bulk}$ (A) and d^2H_{bulk}-$d^{13}C_{16:1}$-oleic/linoleic ratio (B). The d^2H_{bulk}-$d^{18}O_{bulk}$ relationship in the EVOOs is compared with the local meteoric water line (LMWL) and the d^2H-$d^{18}O$ values of waters used for irrigation of olive trees in some regions (1, 4, 6, and 8 in Fig. 1).

describing the relationship between δ^2H and $\delta^{18}O$ in precipitation is the meteoric water line (MWL) (Fig. 2C). We determined the local MWL using the IAEA/GNIP stable isotope data (IAEA/GNIP, 2023) from stations in central-western Argentina and Uruguay based on the latitude and longitude of the olive oil regions. The δ^2H and $\delta^{18}O$ values of irrigation waters (given in Table S4) fell within the local MWL (Fig. 2C), which has a slope (7.64) and intercept (9.7) lower than the global MWL ($\delta^2H = 8 \times \delta^{18}O + 10$; Rozanski et al., 1993) because of the aridity of some studied regions. The δ^2H and $\delta^{18}O$ values in the EVOOs of regions 1–6 and 7–8 define two regression lines with similar slopes but different intercepts ($\delta^2H = 3.56 \times \delta^{18}O$ –239.4 and $\delta^2H = 3.39 \times \delta^{18}O$ –262.7, respectively, $P < 0.01$; Fig. 2D). Similar δ^2H-$\delta^{18}O$ lines have been obtained worldwide for olive oils (Bontempo et al., 2009, 2019) and olive oils and other C_3 and C_4 vegetable oils (Spangenberg, 2016).

3.2. Concentrations of fatty acids in olive oils

The fatty acid (FA) profiles of the studied monovarietal EVOOs from different regions in Argentina and Uruguay are depicted as boxplots in Figs. S2B–G, and a comparison of the average values is shown in Tables 1 and S3. There were few statistically significant ($P > 0.05$) differences in the contents of the main saturated and monounsaturated fatty acids, including palmitic acid (C16:0), stearic acid (C18:0), and oleic acid (C18:1), among the olive oils from the different regions. The concentration of linoleic acid (C18:2) was significantly stronger ($P < 0.05$) in oils from Cerro Largo (region 3) than in those from Maldonado (region 1). This difference can most likely be explained by the distinct predominance of cultivars in these regions. EVOOs produced from the Arbequina cultivar are prevalent in regions 3 and 8 and have consistently lower oleic acid contents and higher palmitic and linoleic acid contents than those from the Mediterranean Basin (Torres et al., 2017). It has also been proposed that lower oleic acid content in monovarietal oils from the Arbequina, Picual, Frantoio, and Coratina cultivars in northern central-western Argentina is linked to higher temperatures during lipid synthesis and oil accumulation (Rondanini, Castro, Searles, & Rousseaux, 2011). Additionally, early harvesting Arbequina has been shown to yield EVOOs with characteristically low oleic acid content (Ceci, Mattar, & Carelli, 2017). The incidence of the Arauco cultivar could also explain the low oleic acid content and oleic/linoleic acid concentration ratio in EVOOs from region 8 (Table 1 and Fig. S2b). This

is in line with the particularly low oleic acid content reported for the Arauco oils from this region (Rondanini et al., 2011). Interestingly, the concentrations of margaric acid (C17:0) were relatively higher in the Uruguayan oils than in the Argentinian oils and were significantly different in oils from Colonia (i.e., region 4 vs. regions 3 and 5–7; Tables 1 and S3). It seems that there are only minor differences among the sites in terms of the concentrations of other minor FAs such as palmitoleic C16:1 and linolenic C18:3 acids, as well as the less abundant C17:1, C20:0, C20:1, and C22:0 acids. However, the concentration ratios of FA (i.e., low oleic/linoleic ratio) and other factors such as the low δ^2H values, can distinguish EVOOs from Mendoza and San Juan (7, 8) from those of other regions. This information is presented in the 3D scatterplot of Fig. 2B, where both variables are plotted versus the $\delta^{13}C_{16:1}$ values. Additionally, the EVOOs from regions 1 and 2 have relatively high oleic/linoleic ratios and δ^2H values (Fig. 2B).

3.3. Carbon isotope composition of fatty acids in olive oils

The δ^{13}C values were determined for the five most abundant FAs. The results are presented with the FAs ordered in biosynthetic order, following the degree of C_2 elongation and unsaturation of the acyl chain: palmitic, palmitoleic, stearic, oleic, and linoleic acids. A comparison of the average δ^{13}C values among the different EVOO regions is presented in Tables 1 and S3, and their distributions are depicted as boxplots in Fig. S2H-I. Clear differences, but not all of which were statistically significant ($P < 0.05$), were detected between the Argentinian and Uruguayan regions, mainly for the δ^{13}C values of palmitic, palmitoleic, and oleic acids. As expected from their biosynthetic link to the same carbon source (photosynthates), the δ^{13}C values of the fatty acids were positively correlated ($P < 0.01$) with the δ^{13}C values of the bulk oil and with each other (Fig. S3). Only the δ^{13}C values of the monounsaturated acids, palmitoleic acids, and oleic acids were strongly correlated with the geoclimatic parameters, which were negatively correlated with latitude, average yearly humidity, and precipitation and positively correlated with longitude, altitude, and mean annual sunshine duration (Fig. S3). The δ^{13}C values of stearic, oleic, and linoleic acids were marginally ($r < 0.4$, $P < 0.05$) negatively correlated with the bulk oil δ^2H values and not with the δ^{18}O values.

We were the first to report trends in the δ^{13}C values of fatty acids in olive and other vegetable oils. We discussed these issues in terms of isotopic fractionation during lipid biosynthesis (i.e., fatty acid synthesis and the formation of acylglycerols) and potential adulteration of the oils (Richter, Spangenberg, Kreuzer, & Leiber, 2010; Spangenberg et al., 1998; Spangenberg & Ogrinc, 2001). We posited that the bulk oil isotopic discriminations between the first biosynthesized fatty acid (C16:0) and the first elongation and unsaturated product (C18:1) would be approximately ±0.5 mUr. On average, these isotope effects seem to be more important in Argentinian and Uruguayan olive oils. The average δ^{13}C values showed the following trend (ANOVA, $F = 46.4$, $P < 0.0001$): δ^{13}C18:0 ≈ δ^{13}C18:2 < δ^{13}C16:0 ≈ δ^{13}C16:1 < δ^{13}C18:1 (Table 1), which are depicted as boxplots in Fig. 3. A similar trend was reported for the δ^{13}C values of the main fatty acids in European and non-European EVOOs (Bontempo et al., 2019). These δ^{13}C differences among the fatty acids integrate the effects associated with isotopic fractionation during fatty acid biosynthesis and the formation of triacylglycerols, coupled with isotopic effects due to the different cultivars and altitudes (and climates) at the growing sites. Here, we evaluate the isotopic fractionation among olive oil fatty acids based on ^{13}C isotope fractionation measured in authentic Argentinian and Uruguayan monovarietal EVOO samples and recent literature on biochemical pathways (Hölzl & Dörmann, 2019; Kazaz, Miray, Lepiniec, & Baud, 2022) and carbon isotope fractionation (Julien et al., 2022) associated with fatty acid biosynthesis.

In plants, chloroplasts are the primary site for de novo fatty acid synthesis, not the cytosol, as in animals. Fatty acids are biosynthesized by repeated groups of reactions catalyzed by fatty acid synthase (FAS) present in the stroma of chloroplasts. In each set of reactions, wherein an isotopic effect may occur, two carbon units of ^{13}C-depleted malonyl-CoA are added to an elongating acyl chain. The nonstatistical distribution of ^{13}C in the photosynthate (i.e., glucose, fructose) and the isotope effects that occur during the formation of acetyl-CoA from pyruvate and its carboxylation catalyzed by acetyl-CoA carboxylase explain the ^{13}C depletion of the methyl (CH_3) position in malonyl-CoA compared to that in acetyl-CoA (Julien et al., 2022). Therefore, the intramolecular ^{13}C

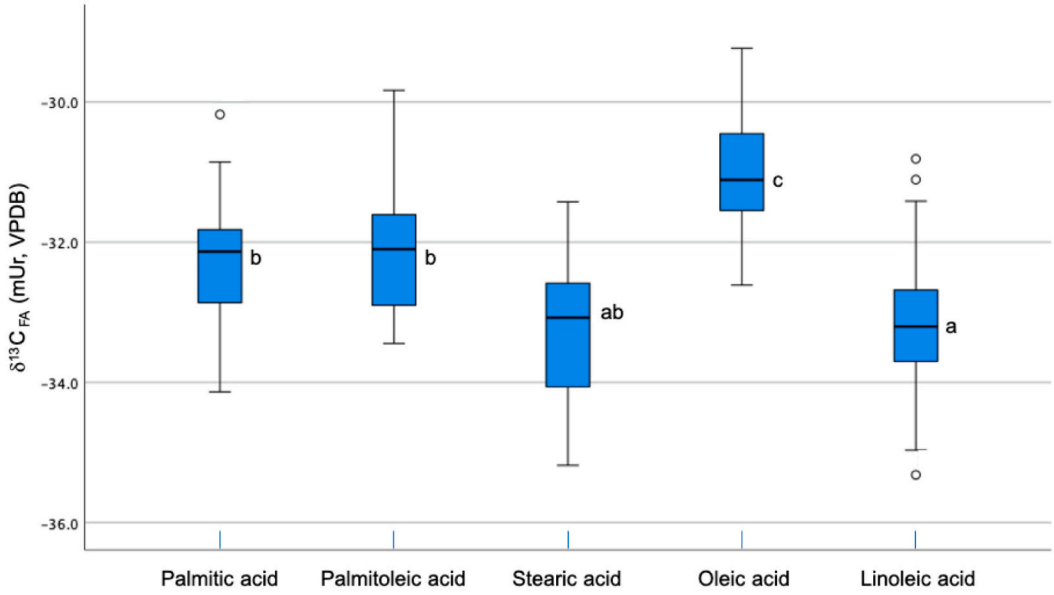

Fig. 3. Boxplots of the d^{13}C values of the individual fatty acids separated from the 43 olive oils from Argentina and Uruguay. The fatty acids are ordered according to the biosynthetic pathway following the C_2 elongation and the degree of unsaturation of the acyl chain. Means that were significantly different based on Tukey HSD test are labeled with different letters.

distribution within fatty acids is characterized by terminal methyl moieties enriched in ^{13}C because they arise from acetyl-CoA, and all even C-atom positions arising from malonyl-CoA are relatively depleted in ^{13}C. The end products of de novo fatty acid synthesis are palmitate and stearate chains (C16:0, C18:0). It could be expected that both fatty acids have similar ^{13}C isotope compositions, as both are produced from a similar metabolic pool. However, our results show that stearate is depleted in ^{13}C (i.e., has a lower $\delta^{13}C$ value) than the C16 homologs and more strongly depleted when is compared to oleate (Fig. 3). These data confirm that elongation and desaturation of the precursor FA chains are most likely are associated with isotopic fractionation associated with branch points coupled with differences in flow, allocation patterns, and enzymatic isotope effects (Julien et al., 2022 and references therein).

Once formed, a stromal soluble Δ9 desaturase readily converts stearate into oleate. This enzyme is very active (Kazaz et al., 2022); therefore, stearate does not accumulate in plastids, and the main products of plastidial fatty acid synthesis are C18:1 and C16:0 (Sánchez & Harwood, 2002). The measured $\delta\ ^{13}C$ values of palmitoleic acid are generally within 1 mUr of the palmitic acid values ($\Delta^{13}C_{16:1-16:0} = \delta^{13}C_{16:1} - \delta^{13}C_{16:0} = +0.12 \pm 1.00$ mUr), suggesting minimal fractionation during the enzymatic desaturation of palmitate.

The C16:0 and C18:1 chains can follow two pathways: they can be used for the synthesis of plastid membrane lipids (called the prokaryotic pathway) or are exported to the endoplasmic reticulum as acyl-CoA esters and incorporated into storage triacylglycerols that may be redistributed to the chloroplast (eukaryotic pathway) (Kazaz et al., 2022; Sánchez & Harwood, 2002). The elongation and desaturation of fatty acid acyl chains occur mainly in the endoplasmic reticulum. Therefore, fatty acids can be desaturated in both the plastid and endoplasmic reticulum by specific fatty acid desaturase enzymes, which most likely induces further isotopic fractionation associated with metabolic branch points, enzymatic reactions, different substrates, and different allocations of substrates and products. The elongation of palmitate, which involves the addition of a further ^{13}C-depleted C_2-unit from malonyl-CoA, results in the production of stearate in the ER. The kinetic fractionation associated with this incomplete enzymatic reaction introduces a ^{13}C-depleted C_2-unit preferentially in ^{12}C-depleted palmitoyl moieties, most likely producing ^{13}C stearate chains, mainly with low $\delta^{13}C$ values. These processes are in line with our data, showing $\Delta^{13}C_{18:0-16:0} = -0.95 \pm 0.91$ mUr (Fig. 3). Stearate may subsequently be desaturated to oleate in the ER. Plants use C18:1 chains bound to phosphatidyl-glycolin to obtain linoleic and linolenic acids (C18:2, C18:3) via Δ12 and Δ15 desaturases (Kazaz et al., 2022). Kinetic isotope effects associated with the desaturation of oleate, with the preferential reaction of isotopically light moieties, would result in the production of ^{13}C-depleted linoleic acid. This ^{13}C depletion is more pronounced in linolenic acid, as shown in rapeseed oils (Richter et al., 2010). Oleic acid would be ^{13}C-enriched during these reactions, which is in line with the measured $\Delta^{13}C_{18:2-18:1}$ of -2.04 ± 1.20 mUr (Fig. 3). A further isotope effect is associated with the hydrolysis of the thioester bond, with the release of fatty acid acyl chain intermediates from acyl carrier proteins, allowing the preferential incorporation of isotopically light fatty acids to produce mono-, di- or tri-acylglycerols as the main lipids in vegetable oils (Julien et al., 2022).

Our data show that understanding the potential natural isotopic fractionation associated with the biosynthesis of fatty acids and acylglycerols is essential to ensure accuracy and robustness when using their isotopic compositions for food authentication and tracing. The observed trend in the $^{13}C/^{12}C$ ratios of the main fatty acids is consistent with the isotopic fractionations associated with their synthesis and assemblage of acylglycerols. This parameter should be considered in authentication studies of extra virgin olive oils.

3.4. Discriminating the geographical origin of Argentinian and Uruguayan olive oils

3.4.1. Unsupervised analysis with PCA

Principal component analysis was used to assess the association of variables and their discriminatory power for EVOO samples. This involved combining variables to form new variables (principal components). The results of the one-way ANOVA (Tables 1 and S3) and Pearson's correlation coefficients (Fig. S3), and presentations in two- and three-dimensional scatterplots (e.g., Fig. 2) were used to select the variables for PCA, which classified and differentiated the Argentinian and Uruguayan EVOO samples. Furthermore, a subset of variables was chosen for the PCA grouping of EVOO regions by visualizing different dimensionality reduction results using 3D scatterplots of loadings and scores. The nine retained variables included the bulk oil isotopes ($\delta^{13}C$, $\delta^{2}H$, $\delta^{18}O$), the $\delta^{13}C$ values of C16:0, C16:1, C18:0, C18:1, and C18:2 fatty acids, and the oleic/linoleic acid concentration ratio. The first three PCA components explained 71.3% of the total variance. A 3D scatterplot of the PCA loadings (Fig. 4A) depicts the groups of correlated variables with greater influence on the components PC1 ($\delta\ ^{13}C_{16:0}$, $\delta\ ^{13}C_{bulk}$, $\delta^{13}C_{18:1}$, $\delta^{13}C_{18:0}$, $\delta^{13}C_{18:2}$, $\delta^{13}C_{16:1}$, in the order of decreasing loading), PC2 ($\delta^{2}H_{bulk}$, oleic/linoleic), and PC3 ($\delta^{18}O_{bulk}$). Examination of the 3D scatterplot of the PCA scores in Fig. 4B reveals that PC1 and PC2 discriminate between olive oils in Uruguayan regions 1–4 and those in Argentinian regions 6–8. Samples from the Salto department in Uruguay plot close to those of Mendoza Province in Argentina (regions 5 and 7, respectively). It seems that the first two PC components grouped and distinguished oils from arid regions (7, 8) influenced by the Pacific Ocean relatively well from those in areas with temperate climates (1–4) affected by the Atlantic Ocean. The scores of PC2 and PC3 (i.e., $\delta^{2}H_{bulk}$, oleic/linoleic, and $\delta^{18}O_{bulk}$ values) separate the samples from Córdoba (region 6) from the others.

3.4.2. Supervised analysis with LDA

The PCA results suggested that the Argentinian and Uruguayan EVOOs can be clustered into three groups that match geoclimatic growing regions. Group 1 comprises regions 7 and 8 (Mendoza and San Juan) in central-western Argentina, group 2 includes region 6 (Córdoba) in central Argentina, and group 3 consists of Uruguayan sites (regions 1–6). The LDA was then used to characterize and differentiate the chemical and isotopic fingerprints of these three groups of oils. The forward stepwise LDA technique was applied, starting with 25 variables, including the bulk and molecular isotopic ratios, fatty acid concentrations, and fatty acid concentration ratios (listed in Table 1). The variable subset was selected via stepwise statistics, using Wilks' lambda as the selection criterion and the *F*-statistic to determine the significance of the lambda changes when a new variable was tested. At each step, the variable that minimized the overall Wilks' lambda factor, a parameter ranging from 1.0 for no discriminatory power to 0.0 for perfect discriminatory power, was retained. The obtained final selection consisted of a subset of four variables with high discriminating power, including $\delta^{2}H_{bulk}$, $\delta^{18}O_{bulk}$, $\delta^{13}C_{16:1}$, and $\delta^{13}C_{18:2}$. The discriminant functions determined (Fig. 4C) by maximizing the variances of the variables between groups (categories) and by minimizing those within groups led to significant differences between the three groups of regions, i.e., two Argentinian regions and Uruguay as the third region, as depicted in the scatterplot in Fig. 4D. Functions 1 and 2 explained 90.6% and 9.4% of the variance, respectively, and their Wilk's values were 0.087 and 0.613 ($P < 0.001$), respectively. The recognition ability (correct assignment of the samples to the groups) was calculated at 95.3%. One oil from central-western Argentina (group 1, Mendoza and San Juan) was incorrectly assigned to Córdoba (group 2, central Argentina), and one Uruguayan oil (group 3) was assigned to central-western Argentina. The predictive ability of the stepwise LDA model was evaluated by the leave-one-out cross-validation (LOOCV) method, which yielded 93.0% of cross-validated grouped cases correctly

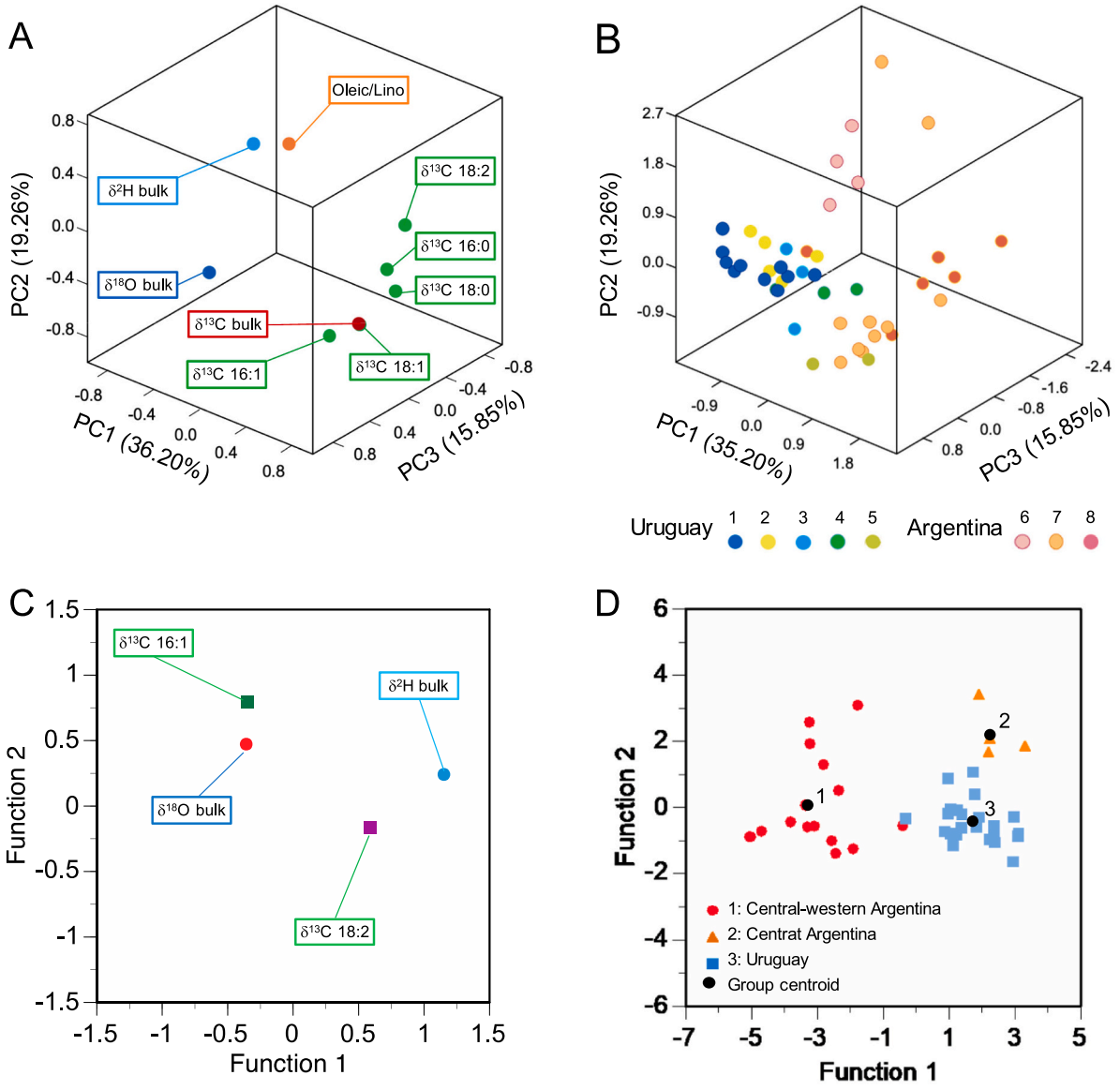

Fig. 4. Three-dimensional scatter plots of loadings and scores of PCA (A, B) and classification function coefficients and scores from LDA (C, D) performed on 43 EVOO samples from Argentina and Uruguay. PC1, PC2, and PC3 explain 71.32% of the total variance of seven stable isotope variables and oleic/linoleic concentration ratios. The colored symbols for the PC scores (C) are similar to those used in Figs. 1 and 2. The results of LDA based on four stepwise selected variables show that 95.3% of the original grouped samples (Group 1: sites 7 and 8, Group 2: site 6, and Group 3: sites 1–5-; see site locations in Fig. 1) were correctly classified and that 93.0% samples cross-validated by the leave-one-out procedure were correctly classified.

classified, indicating good performance. The results confirmed that combined bulk oil isotopic compositions (i.e., δ^2H and δ^{18}O values) and δ^{13}C values of individual fatty acids (i.e., $\delta^{13}C_{16:1}$ and $\delta^{13}C_{18:2}$ values) provide useful information for the classification of Argentinian and Uruguayan olive oils. Finally, when performing LDA with the nine variables selected for PCA, the recognition ability increased to 100%, but the predictive ability checked by LOOCV decreased to 88.4%. The reduced number of variables used in the stepwise LDA model led to the best clustering of oil samples and a reliable increase in the relative percentage of the original grouped samples correctly classified, suggesting that some variables (e.g., concentrations and most derived parameters from fatty acids) are poorly correlated and mask or conceal the discriminatory power of other variables (i.e., δ^2H_{bulk}, $\delta^{18}O_{bulk}$, and fatty acid δ^{13}C values).

3.4.3. General linear model: Geographic origin vs. variety

Two-way ANOVA (GLM) was performed to evaluate the impact of cultivar on fatty acid composition and isotopic ratios as indicators of geographical origin. The model included the average values of all variables—isotope ratios in bulk oils and individual fatty acids, their concentrations, and concentration ratios—and the influences of two factors including cultivar and geographical origin, and the interaction of both factors. The considered cultivars were the most common olive varieties in the sample set (i.e., Arauco, Arbequina, and Frantoio). The geographical regions considered were those that contained sufficient samples of the oil varieties (i.e., centra-western Argentina and Uruguay). Multiple comparisons among means were performed with Tukey's method ($P < 0.05$). The GLM results indicate that geographical origin (central-western Argentina vs. Uruguay) was highly significant ($P < 0.002$) for δ^2H_{bulk}, was significant ($P < 0.05$) for δ^{13}C values of

Table 2
General linear model *P* values of the geographical and varietal factors[a] affecting the isotopes and and fatty acid composition of the Argentinian and Uruguayan olive oils based on PCA and LDA scores.

	P-value		
	Origin effect	Cultivar effect	Origin*Cultivar Interaction
PCA C1	0.89	0.38	0.30
PCA C2	<0.001[b]	0.78	0.12
PCA C3	0.19	0.19	0.34
LDA F1	<0.001[b]	0.90	0.42
LDA F2	0.59	0.16	0.82

[a] Geographical origin of EVOOs produced in farms in central-western Argentina and Uruguay from olive cultivars Arauco, Arbequina, and Frantoia.
[b] Value significant at $P < 0.05$.

palmitoleic acid, and concentrations of margaric and stearic acids and had a marginal effect ($0.05 < P < 0.1$) on PUFA/SFA concentration ratios (Table S5). The cultivar effect was by far the most significant for palmitoleic acid concentrations ($P = 0.004$) and $\delta^{13}C$ values of oleic acid ($P = 0.02$) and was marginal ($0.05 < P < 0.1$) for $\delta^{13}C_{bulk}$ values, concentrations of palmitic acid, oleic acid, SFAs, MUFAs, and linoleic/linolenic ratios. The lack of significant interaction between geographical origin and cultivar or all variables indicates that the cultivar effects on the measured bulk and molecular isotopes and fatty acid profiles seem to be the same for olive oils from northwestern Argentina or Uruguay. Finally, the effects of geographical origin and cultivar on the scores of the three PCA components and two LDA functions were investigated. The effect of geographical origin was highly significant for PCA C2 and LDA F1 (Tables 2 and S5). This finding was expected because the growing site was the categorical dependent variable. However, the variety (cultivar) had marginal but not statistically significant effects on PCA C3 and LDA F2 ($P = 0.19$ and 0.16, respectively). The geographic origin × cultivar interaction is not significant for the PCA and LDA scores.

4. Conclusions

Here, we report for the first time the bulk ($^2H/^1H$, $^{18}O/^{16}O$, and $^{13}C/^{12}C$) and molecular ($^{13}C/^{12}C$) stable isotope ratios and fatty acid profiles of 43 authentic monovarietal virgin olive oils produced in different regions of Argentina and Uruguay and their classification by geographical origin/provenance using chemometrics. The samples were chosen to represent the major olive cultivars on farms along a transect from the coastal lowland of southeastern Uruguay influenced by the Atlantic Ocean, passing through the lowland grasslands and agricultural fields of eastern Córdoba in central Argentina to the fertile valleys of pre-Andean highlands in the northwestern Argentinian provinces of Mendoza and San Juan, which are influenced by the Pacific Ocean. Significant differences were observed between the δ^2H_{bulk}, $\delta^{18}O_{bulk}$, $\delta^{13}C_{bulk}$, and $\delta^{13}C_{18:1}$ values of oils from northwestern Argentina, central Argentina, and Uruguay. The type of soil water (rainwater, irrigation with tap water, groundwater, or their combination) available to the olive tree seems to impact the δ^2H_{bulk} and $\delta^{18}O_{bulk}$ values of the oils. The differences in the $\delta^{13}C$ values of the individual fatty acids in the authentic extra virgin olive oils from this study are explained by isotopic fractionation associated with the biosynthesis of fatty acids and the formation of alkylglycerols. Potential differences due to cultivars appear to be neutralized by geoclimatic conditions and cultivation practices. The trend in the $^{13}C/^{12}C$ ratios of the individual fatty acids in the extra virgin olive oils from this study: $\delta^{13}C$-stearate ≈ $\delta^{13}C$-linoleate < $\delta^{13}C$-palmitic ≈ $\delta^{13}C$-palmitoleic < $\delta^{13}C$-oleic acid, is consistent with the isotopic fractionations associated with their synthesis and assemblage of acylglycerols. The trend in the $^{13}C/^{12}C$ ratios, therefore, may be a parameter that needs to be considered in authentication and tracing studies of extra virgin olive oils. The results of this study show that combined stable isotope ratios of bulk ($^2H/^1H$ and $^{18}O/^{16}O$) and fatty acids ($^{13}C/^{12}C$) and chemometrics may be used for geographic origin differentiation among olive oils from Argentina and Uruguay.

CRediT authorship contribution statement

Jorge Enrique Spangenberg: Conceptualization, Methodology, Data curation, Formal analysis, Visualization, Writing – original draft, Writing – review & editing. **Irene Lantos:** Conceptualization, Methodology, Writing – review & editing.

Declaration of competing interest

The authors declare that they have no known competing financial interests or personal relationships that could have appeared to influence the study reported in this paper.

Data availability

All data for this paper are within the manuscript and its Supplementary Information.

Acknowledgments

The authors are grateful to all those who provided olive oil samples and information on their farms and agricultural practices: María Lourdes Toujas, Martín Robaina (Lote 8), Ana Sala (Olivares Salteños), Juan Borda (O33), Jorge Roimiser (La Primavera), Gonzalo and Laura Aguirre (Olivares Santa Laura), Víctor Rodríguez (Nuevo Manantial, Agroland SA), Esteban Santipolio (Tutuna), Juan Pablo Castellano (Trilogía), Pablo Geier (Olium), and INTA (San Juan). The stable isotope facilities at the Institute of Earth Surface Dynamics (IDYST) are supported by the Faculty of Environmental Geoscience of the University of Lausanne and the Swiss National Science Foundation.

Appendix A. Supplementary data

Supplementary data to this article can be found online at https://doi.org/10.1016/j.foodchem.2024.139194.

References

Angerosa, F., Bréas, O., Contento, S., Guillou, C., Reniero, F., & Sada, E. (1999). Application of stable isotope ratio analysis to the characterization of the geographical origin of olive oils. *Journal of Agricultural and Food Chemistry, 47*(3), 1013–1017.

Aramendía, M. A., Marinas, A., Marinas, J. M., Sánchez, E., Urbano, F. J., Guillou, C., … Rallo, L. (2010). A nuclear magnetic resonance (^1H and ^{13}C) and isotope ratio mass spectrometry ($\delta^{13}C$, δ^2H and $\delta^{18}O$) study of Andalusian olive oils. *Rapid Communications in Mass Spectrometry, 24*, 1457–1466.

Banco, A., Trentacoste, E., & Monasterio, R. P. (2021). Characterization of virgin olive oils from Spanish olive varieties introduced in Mendoza, Argentina, and their comparison with the autochthonous variety. *Journal of the Science of Food and Agriculture, 101*(2), 518–524.

Bontempo, L., Camin, F., Larcher, R., Nicolini, G., Perini, M., & Rossmann, A. (2009). Coast and year effect on H, O and C stable isotope ratios of Tyrrhenian and Adriatic Italian olive oils. *Rapid Communications in Mass Spectrometry, 23*(7), 1043–1048.

Bontempo, L., Paolini, M., Franceschi, P., Ziller, L., García-González, D. L., & Camin, F. (2019). Characterisation and attempted differentiation of European and extra-European olive oils using stable isotope ratio analysis. *Food Chemistry, 276*, 782–789.

Borges, T. H., Pereira, J. A., Cabrera-Vique, C., Lara, L., Oliveira, A. F., & Seiquer, I. (2017). Characterization of Arbequina virgin olive oils produced in different regions of Brazil and Spain: Physicochemical properties, oxidative stability and fatty acid profile. *Food Chemistry, 215*, 454–462.

Brand, W. A., & Coplen, T. B. (2012). Stable isotope deltas: Tiny, yet robust signatures in nature. *Isotopes in Environmental and Health Studies, 48*(3), 393–409.

Camin, F., Larcher, R., Nicolini, G., Bontempo, L., Bertoldi, D., Perini, M., Schlicht, C., Schellenberg, A., Thomas, F., Heinrich, K., Voerkelius, S., Horacek, M., Ueckermann, H., Froeschl, H., Wimmer, B., Heiss, G., Baxter, M., Rossmann, A., & Hoogewerff, J. (2010). Isotopic and elemental data for tracing the origin of European olive oils. *Journal of Agricultural and Food Chemistry, 58*(1), 570–577.

Camin, F., Larcher, R., Perini, M., Bontempo, L., Bertoldi, D., Gagliano, G., Nicolini, G., & Versini, G. (2010). Characterisation of authentic Italian extra-virgin olive oils by

stable isotope ratios of C, O and H and mineral composition. *Food Chemistry, 118*(4), 901–909.
Casadei, E., Valli, E., Panni, F., Donarski, J., Gubern, J. F., Lucci, P., … Toschi, T. G. (2021). Emerging trends in olive oil fraud and possible countermeasures. *Food Control, 124*, Article 107902.
Ceci, L. N., Mattar, S. B., & Carelli, A. A. (2017). Chemical quality and oxidative stability of extra virgin olive oils from San Juan province (Argentina). *Food Research International, 100*, 764–770.
Commission Regulation (EC) No 702/2007 of 21 June 2007 amending Commission Regulation (EEC) No 2568/91 on the characteristics of olive oil and olive-residue oil and on the relevant methods of analysis, Annex XA. Official Journal of the European Union, L 161/11–27.
Diez, C. M., Trujillo, I., Martinez-Urdiroz, N., Barranco, D., Rallo, L., Marfil, P., & Gaut, B. S. (2015). Olive domestication and diversification in the Mediterranean Basin. *New Phytologist, 206*(1), 436–447.
Hölzl, G., & Dörmann, P. (2019). Chloroplast lipids and their biosynthesis. *Annual Review of Plant Biology, 70*, 51–81.
Iacumin, P., Bernini, L., & Boschetti, T. (2009). Climatic factors influencing the isotope composition of Italian olive oils and geographic characterisation. *Rapid Communications in Mass Spectrometry, 23*, 448–454.
IAEA/GNIP. (2023). *Global network of isotopes in precipitation*. The GNIP Database. Accessible at https://nucleus.iaea.org/wisel.
Jobbágy, E. G., Nosetto, M. D., Villagra, P. E., & Jackson, R. B. (2011). Water subsidies from mountains to deserts: Their role in sustaining groundwater-fed oases in a sandy landscape. *Ecological Applications, 21*(3), 678–694.
Julien, M., Zhao, Y., Ma, R., Zhou, Y. P., Nakagawa, M., Yamada, K., … Gilbert, A. (2022). Re-evaluation of the ^{13}C isotope fractionation associated with lipids biosynthesis by position-specific isotope analysis of plant fatty acids. *Organic Geochemistry, 174*.
Kazaz, S., Miray, R., Lepiniec, L., & Baud, S. (2022). Plant monounsaturated fatty acids: Diversity, biosynthesis, functions and uses. *Progress in Lipid Research, 85*.
Körner, C., Farquhar, G. D., & Wong, S. C. (1991). Carbon isotope discrimination by plants follows latitudinal and altitudinal trends. *Oecologia, 88*, 30–40.
Ministerio de Ganadería, Agricultura y Pesca. (2020). Censo de productores de olivos 20202. DIEA. Serie Trabajos Especiales N° 364. Uruguay. https://www.gub.uy/ministerio-ganaderia-agricultura-pesca/datos-y-estadisticas/estadisticas/diea-presenta-informe-sobre-censo-productores-olivos-2020.
O'Leary, M. H., Madhavan, S., & Paneth, P. (1992). Physical and chemical basis of carbon isotope fractionation in plants. *Plant, Cell and Environment, 15*, 1099–1104.
Paolini, M., Bontempo, L., & Camin, F. (2017). Compound-specific $\delta^{13}C$ and $\delta^{2}H$ analysis of olive oil fatty acids. *Talanta, 174*, 38–43.
Richter, E. K., Spangenberg, J. E., Kreuzer, M., & Leiber, F. (2010). Characterization of rapeseed (*Brassica napus*) oils by bulk C, O, H, and fatty acid C stable isotope analyses. *Journal of Agricultural and Food Chemistry, 58*, 8048–8055.
Roden, J. S., Lin, G. G., & Ehleringer, J. R. (2000). A mechanistic model for interpretation of hydrogen and oxygen isotope ratios in tree-ring cellulose. *Geochimica et Cosmochimica Acta, 64*(1), 21–35.
Rondanini, D. P., Castro, D. N., Searles, P. S., & Rousseaux, M. C. (2011). Fatty acid profiles of varietal virgin olive oils (*Olea europaea* L.) from mature orchards in warm arid valleys of northwestern Argentina (La Rioja). *Grasas y Aceites, 62*(4), 399–409.
Rozanski, K., Araguás-Araguás, L., & Gonfiantini, R. (1993). Isotopic patterns in modern global precipitation. *Climate change in continental isotopic records. Geophysical Monograph, 78*, 1–36.
Sánchez, J., & Harwood, J. L. (2002). Biosynthesis of triacylglycerols and volatiles in olives. *European Journal of Lipid Science and Technology, 104*(9–10), 564–573.
Schimmelmann, A., Qi, H. P., Dunn, P. J. H., Camin, F., Bontempo, L., Potocnik, D., … Coplen, T. B. (2020). Food matrix reference materials for hydrogen, carbon, nitrogen, oxygen, and sulfur stable isotope-ratio measurements: Collagens, flours, honeys, and vegetable oils. *Journal of Agricultural and Food Chemistry, 68*(39), 10852–10864.
Schmidt, H. L., Werner, R. A., & Eisenreich, W. (2003). Systematics of ^{2}H patterns in natural compounds and its importance for the elucidation of biosynthetic pathways. *Phytochemistry Reviews, 2*, 61–85.
Schmidt, H. L., Werner, R. A., & Rossmann, A. (2001). O-18 pattern and biosynthesis of natural plant products. *Phytochemistry, 58*(1), 9–32.
da Silveira Lobo Sternberg, L. (1989). Oxygen and hydrogen isotope ratios in plant cellulose: Mechanisms and applications. In *Stable isotopes in ecological research* (pp. 124–141). New York, NY: Springer. https://doi.org/10.1007/978-1-4612-3498-2_9.
Spangenberg, J. E. (2012). Caution on the storage of waters and aqueous solutions in plastic containers for hydrogen and oxygen stable isotope analysis. *Rapid Communications in Mass Spectrometry, 26*(22), 2627–2636.
Spangenberg, J. E. (2016). Bulk C, H, O, and fatty acid C stable isotope analyses for purity assessment of vegetable oils from the southern and northern hemispheres. *Rapid Communications in Mass Spectrometry, 30*(23), 2447–2461.
Spangenberg, J. E., Dold, B., Vogt, M. L., & Pfeifer, H. R. (2007). Stable hydrogen and oxygen isotope composition of waters from mine tailings in different climatic environments. *Environmental Science & Technology, 41*(6), 1870–1876.
Spangenberg, J. E., Macko, S. A., & Hunziker, J. (1998). Characterization of olive oil by carbon isotope analysis of individual fatty acids: Implications for authentication. *Journal of Agricultural and Food Chemistry, 46*, 4179–4184.
Spangenberg, J. E., & Ogrinc, N. (2001). Authentication of vegetable oils by bulk and molecular carbon isotope analyses - with emphasis on olive oil and pumpkin seed oil. *Journal of Agricultural and Food Chemistry, 49*, 1534–1540.
Torres, M., Pierantozzi, P., Searles, P., Rousseaux, M. C., Garcia-Inza, G., Miserere, A., … Maestri, D. (2017). Olive cultivation in the southern hemisphere: Flowering, water requirements and oil quality responses to new crop environments. *Frontiers in Plant Science, 8*.
Visciano, P., & Schirone, M. (2021). Food frauds: Global incidents and misleading situations. *Trends in Food Science & Technology, 1140*, 424–442.
Yakir, D., & DeNiro, M. J. (1990). Oxygen and hydrogen isotope fractionation during cellulose metabolism in *lemma gibba* L. *Plant Physiology, 93*(1), 325–332.